Investigation of the *trans* Influence in Transition-metal Nitride Complexes†

Paul D. Lyne[a] **and D. Michael P. Mingos***[,b]
[a] *Physical and Theoretical Chemistry Laboratory, South Parks Road, Oxford OX1 3QZ, UK*
[b] *Department of Chemistry, Imperial College of Science, Technology and Medicine, South Kensington, London SW7 2AY, UK*

Approximate density functional theory calculations have been used to investigate the *trans* influence in five- and six-co-ordinate transition-metal nitride complexes. The geometries of $[OsNX_4]^-$ (X = Cl, Me or SMe) and $[OsNCl_5]^{2-}$ were optimized in the C_{4v} point group. The agreement between calculated and experimental geometric parameters is very good. By employing the transition-state method the relative effects of steric and electronic factors on the *trans* influence in these complexes was quantitatively assessed. It is found that the electronic stabilization is greater than the steric stabilization for five- and six-co-ordinate complexes. The origin of the electronic stabilization was identified. The diverse reactivities of $[OsNX_4]^-$ may be rationalized by a comparison of the frontier orbitals of these complexes. The analogous nitrosyl complex $[Ru(NO)Cl_5]^{2-}$ does not exhibit a *trans* influence on the chloride *trans* to the nitrosyl group. This has been accounted for by considering the electronic structure of this complex.

In 1966 Pidcock, *et al.*[1] considered the NMR coupling constants of the Pt–P bond in a series of twenty five platinum complexes, and attributed the large range to the variability of the bond length. They coined the term '*trans* influence' to describe the tendency of a ligand to weaken the bond *trans* to itself. The *trans* influence, an equilibrium phenomenon, is to be distinguished from the *trans* effect which describes the tendency of a ligand to influence the rate of ligand substitution of a ligand *trans* to itself. This was not by any means the first observation of the *trans* influence, but the first time that a clear distinction was made between equilibrium and kinetic effects. The *trans* influence can be detected in many ways. The most obvious is the observation of bond lengths and geometrical distortions in the crystal structure. Similarly, bond weakening/lengthening may be detected by observing the values of vibrational frequencies and NMR coupling constants. For a summary of the *trans* influence and its structural consequences the reader is directed to reviews by Appleton *et al.*[2] and Nugent and Mayer.[3]

There have been several theoretical discussions of the *trans* influence and effect. As early as 1935 Grinberg[4] proposed an explanation based on polarization theory. An easily polarizable ligand induces a build-up of negative charge on the metal which is directed towards the *trans* position and an incoming ligand at the *trans* position is repelled by the dipole on the metal. The electrostatic viewpoint was improved upon by Syrkin,[5] who included hybridization at the metal to explain the *trans* effect. Chatt *et al.*[6] and Orgel[7] have interpreted the *trans* effect as being due to a strong π interaction between the *trans*-directing ligand and the metal. When two ligands are located *trans* to each other, they compete for the same metal valence orbitals. If one ligand has a larger overlap with these orbitals then there is a diminution in the overlap between the metal and the *trans* ligand.

The *trans* influence and effect have been treated formally within a molecular orbital framework by Shustorovich *et al.*[8] and Burdett and Albright[9] using perturbation theory. They demonstrated that in a linear MLL′ system it is energetically unfavourable for the ligands to share the same metal orbital. If the ligands are forced to share the same metal orbitals there is a differential weakening of one of the metal–ligand bonds.

Electronic arguments are not the only ones proposed in the literature to account for the *trans* influence. In a paper presenting the synthesis and structure of the $K_2[OsNCl_5]$ complex, Bright and Ibers[10] invoked steric arguments to account for the lengthening of the Os–Cl bond *trans* to the nitride ligand and the angular distortion of the *cis* Os–Cl bonds. The short metal–nitride distance causes *cis* chlorides to be displaced away towards the *trans* chloride. Consequently, the *trans* chloride is sterically repelled by the *cis* chlorides and so the bond between the *trans* chloride and the metal lengthens. This steric distortion is illustrated in Scheme 1. Ibers and co-workers[11,12] performed a crystallographic study of $ReNCl_2(PR_3)_2$ (R_3 = Ph_3 or Et_2Ph) systems that supported the steric view of the *trans* influence.

In this paper the relative effects of steric and electronic factors on the *trans* influence in transition-metal nitrido complexes are investigated.

Computational Details

Molecular Orbital Calculations.—All calculations were based on approximate density functional theory (DFT) (see Parr and Yang[13] for an extensive treatment, and Ziegler[14] for a review of the theory and current implementation methods) within the

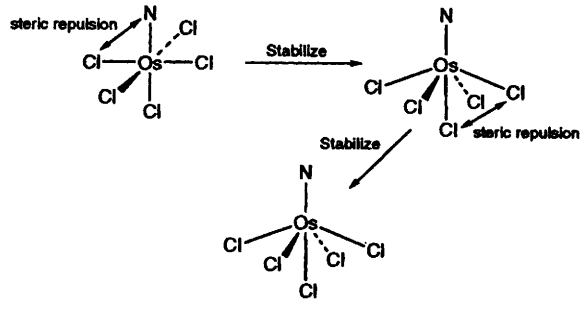

Scheme 1 The weakening of *trans* chloride due to steric interactions

† *Non-SI unit employed:* eV ≈ 1.60 × 10^{-19} J.

Local Density Approximation,[15-17] LDA. The exchange factor, α_{ex}, was taken as 0.7 and the correlation potential was that of Stoll *et al.*[18,19] in the parameterization by Vosko, *et al.*[20] The calculations were performed utilizing the vectorized version of the Hartree–Fock–Slater linear combination of atomic orbitals (HFS-LCAO) program suite, ADF, developed by Baerends *et al.*,[21,22] and vectorized by Ravenek.[23] The numerical integration procedure applied was based on the scheme developed by Boerrigter *et al.*[24] The *n*s, *n*p, *n*d, (*n* + 1)s and (*n* + 1)p shells of osmium were represented by a triple-ζ-Slater-type orbital (STO) basis set.[25,26] A double-ζ-STO basis set was employed for the *n*s and *n*p shells of the main-group elements. For nitrogen and carbon this basis was augmented by a single 3d STO function; for chlorine and sulfur by a 4d STO function, and for hydrogen a 2p STO function was used for polarization. For all atoms electrons in lower shells were considered as core and treated according to the frozen-core approximation of Baerends *et al.*[21] On osmium the core orbitals comprised the 1s2s2p3s3p3d4s4p4d4f orbitals; on carbon and nitrogen the 1s orbital was treated as core and for sulfur and chlorine the 1s2s2p orbitals were treated as core. An auxiliary set[27] of s, p, d, f and g STO functions, centred on all nuclei, was used in order to fit the molecular density and present Coulomb and exchange potentials accurately in each self-consistent field (SCF) cycle. This is a standard feature of implementation of DFT and is used to reduce the computation time. The electron density is expanded as in equation (1) where

$$\rho \longrightarrow \tilde{\rho} = \sum_i a_i f_i(r) \qquad (1)$$

$f_i(r)$ are the auxiliary fit functions and the coefficients a_i are determined in a least-squares-fitting procedure.[14] The total energy of the system was calculated according to equation (2).[14]

$$E = E_{HFS} + E_c + E_x^{NL} + E_c^{NL} \qquad (2)$$

Here E_{HFS} is the total statistical energy expression for the Hartree–Fock–Slater method, while E_c, E_x^{NL} and E_c^{NL} are additional correction terms. The first, E_c, is a correlation potential for electrons of different spins in Vosko's parameterization, the second E_x^{NL} is a non-local exchange correction proposed by Becke,[28] and E_c^{NL} is a non-local correction to the correlation, proposed by Perdew.[29]

Energy Decomposition Scheme.—The total bonding energies presented were evaluated using an energy decomposition scheme based on the generalized transition state method developed by Ziegler and Rauk.[30] This method decomposes the total bonding energy of a system into steric and electronic components. A brief description of the scheme employed is presented here. The reader is referred to the original papers of Ziegler and co-workers[30-33] for explicit details of the transition-state method, and to refs. 34–38 for a sample of recent applications of the method to studies of the energetics of chemical systems.

The transition-state method considers the molecule of interest to be comprised of fragments, which may be either atoms or molecular fragments. The change in energy, ΔE, associated with the interaction between these fragments is given in equation (3) where ΔE_{steric} refers to the change in steric

$$\Delta E_b = -(\Delta E_{steric} + \Delta E_{el}) \qquad (3)$$

interaction energy and ΔE_{el} to the change in electronic interaction energy. Essentially, the latter term represents the interaction energies between the orbitals of the various fragments. The term ΔE_{steric} may be further decomposed as in equation (4). The first term, ΔE_{elst} represents the change in electrostatic interaction energy between the fragments, the second ΔE_{dlxc} corresponds to the change in exchange correlation energy while the final term ΔE_{exrp} refers to the change in exchange repulsion energy; ΔE_{exrp} is directly related to the so-called 'four-electron two-orbital' interactions. The term ΔE_{el} comprises the interaction energies of the orbital irreducible representation of the pertinent symmetry point group(Γ), equation (5).

$$\Delta E_{steric} = \Delta E_{elst} + \Delta E_{dlxc} + \Delta E_{exrp} \qquad (4)$$

$$\Delta E_{el} = \sum_\Gamma \Delta E^\Gamma \qquad (5)$$

The energy decomposition scheme outlined here has been successfully applied to studying bond strengths[34] and steric interactions[35] and is well suited for the current study of the *trans* influence. All the bond-energy calculations included gradient corrections developed by Becke[28] and Perdew.[29] An energy-decomposition scheme will depend on the fragment decomposition employed and thus the numerical values of the energy components will vary with alternative fragment decompositions. In the cases studied in this paper energy analyses were performed on the whole molecule for each conformer studied.

Geometry Optimizations.—All the calculations were performed in C_{4v} symmetry. This is not an unreasonable limitation since most of the molecules have been structurally characterized as having approximate C_{4v} symmetry. Full optimizations within C_{4v} symmetry were performed for each molecule, unless otherwise stated. The geometry-optimization procedure was based on the method developed by Versluis and Ziegler.[39]

Results and Discussion

There are two structural features associated with the *trans* influence in six-co-ordinate transition-metal nitrido complexes. First, there is a weakening of the bond between the metal and the *trans* ligand. Secondly, the equatorial ligands bend away from the nitride ligand. The latter feature is also present in analogous five-co-ordinate systems. Since the electronic structures of five- and six-co-ordinate complexes should be similar, it was decided that the electronic and structural properties of five-co-ordinate nitrido complexes are a convenient starting point for our study of the *trans* influence in nitrido complexes.

Five-co-ordinate Complexes.—There are now several examples of five-co-ordinate transition-metal nitrido complexes. The majority of these are of the Group VI–VIII metals.[3,40] All have pseudo-square-pyramidal geometries with the basal ligands distorted away from the nitride. In this section we focus our attention on $[OsNX_4]^-$ complexes, where X = Cl, Me or SMe. These ligands were chosen to investigate the influence of the electronic nature of X on the *trans* influence in these complexes. There are several examples of crystallographically characterized complexes containing these ligands. The geometric data associated with these complexes are summarized in Table 1. It may be seen that the extent of angular distortion is reasonably consistent. When X is a halide ligand, the average N–M–X angle is 103.7°. When X is a thiolate or alkyl ligand, N–M–X is slightly larger. In the $[MNX_4]^-$ complexes given in Table 1 the M≡N distance has an average value of 161 pm.

Geometric structures. We have optimized the geometries of $[OsNX_4]^-$ (X = Cl, Me or SMe). Since five-co-ordinate transition-metal nitrido complexes are invariably square pyramidal, all optimizations were performed in C_{4v} symmetry. The general structure of the optimized compounds is shown in Fig. 1 and the calculated geometric parameters are given in

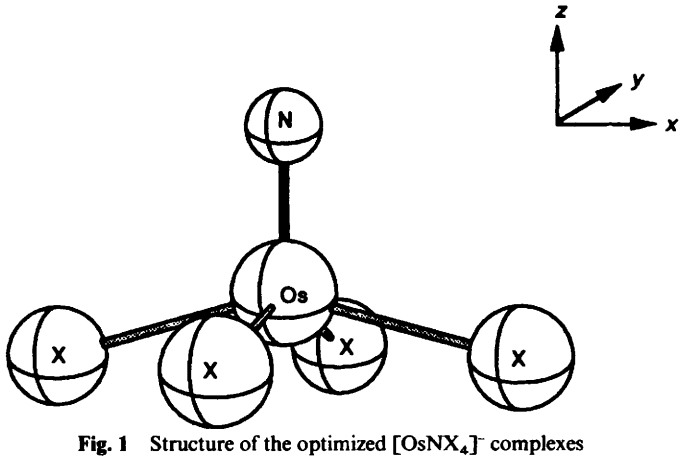

Fig. 1 Structure of the optimized $[OsNX_4]^-$ complexes

Table 1 Geometric data for some $[MNX_4]^-$ complexes

Compound	M≡N/pm	N–M–X/°	Ref.
$[MoNCl_4]^-$	163.7	103.1	41
$[TcNCl_4]^-$	158.1	103.3	42
$[ReNBr_4]^-$	162.0	103.0	43
$[ReNCl_2(PPh_3)_2]$	160.2	98.9	12
$[RuNCl_4]^-$	157.0	104.6	44
$[OsNCl_4]^-$	160.4	104.5	45
$[TcN(S_2CNEt_2)_2]$	160.4	108.1	46
$[RuNMe_4]^-$	158.0	110.4	48
$[OsN(CH_2SiMe_3)_4]^-$	163.1	108.0	47
$[MoN(N_3)_4]^-$	163.0	99.5	49

Table 2 Calculated geometric data for $[OsNX_4]^-$ complexes, where X = Cl, Me or SMe

Compound	M≡N/pm	M–X/pm	N–M–X/°
$[OsNCl_4]^-$	165.2	242.2	104.81
$[OsNMe_4]^-$	165.7	219.3	110.67
$[OsN(SMe)_4]^-$	165.4	241.8	107.90

Table 2. Comparison of the data in Tables 1 and 2 shows that there is very good agreement with experimental structures. The experimental geometric trends as the ligand X is varied are reproduced in the optimized geometries. In particular the angular distortion of the basal ligands is greatest when X = Me and least when X = Cl.

Molecular-orbital (MO) calculations. A molecular-orbital analysis of transition-metal five-co-ordination has been presented previously by Rossi and Hoffmann.[50] It focused primarily on the σ-bonding trends in square-pyramidal complexes. In addition, the site preferences of π-donor and -acceptor ligands in such complexes were discussed. It was concluded that the extent of interaction of a π donor located at the apical position of a square pyramid is directly related to the angle of pyramidalization, θ, defined in **I**. Cylindrical π donors located at the apical position of a square pyramid have stronger interactions with the metal orbitals when θ > 90°. In this section a detailed study of the molecular orbitals of $[OsNCl_4]^-$ using approximate density functional theory is presented. The consequences for the orbital interactions of opening the angle θ from 90 to 104.8° (the value of θ in the optimized structure) are explored. The electronic structures of the $[OsNX_4]^-$ complexes are very similar, therefore for the purposes of this discussion we initially focus our attention on the electronic structure of $[OsNCl_4]^-$. The effect of varying the ligands X is discussed later.

In Fig. 2 the key molecular orbitals of $[OsNCl_4]^-$ with θ = 90.0° are shown. The HOMO of the 'flat' (θ = 90.0°) square

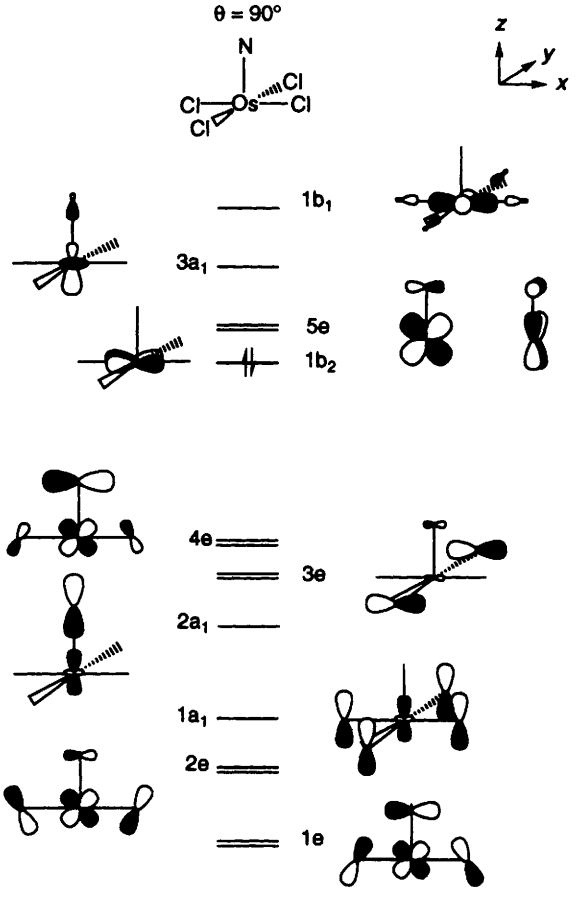

Fig. 2 Selected molecular orbitals of $[OsNCl_4]^-$. The highest occupied molecular orbital (HOMO) is indicated by an electron pair; for convenience, only one component of orbitals, 4e, 3e, 2e and 1e is shown

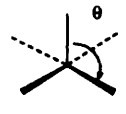

I

pyramid is the $1b_2$ orbital, which is localized on the d_{xy} orbital of osmium. In the C_{4v} point group, symmetry dictates that the d_{xy} orbital (adopting the coordinate system shown in Fig. 1) only interacts with the p_x and p_y orbitals of the basal chlorides. All the valence orbitals of nitrogen and the σ orbitals of the chlorides lie in the nodal planes of the d_{xy} orbital. Above the $1b_2$

orbital lie four other molecular orbitals which are localized mainly on osmium. The 5e orbitals correspond to antibonding interactions between the nitrido π orbitals and the d_{xz} and d_{yz} orbitals of osmium. The $3a_1$ orbital is localized predominantly on the nitrogen and osmium atoms. It is antibonding with respect to the metal and the nitride, but the overlap between them is reduced by a hybridization of the metal orbital away from this ligand. The hybridization of this orbital makes it function as the primary acceptor orbital when an additional ligand is introduced into the co-ordination sphere. The $1b_1$ orbital corresponds to antibonding interactions between the $d_{x^2-y^2}$ orbital of osmium and the σ orbitals of the chlorides. The relative order of these energy levels is in agreement with previous calculations.[51,52] Since $[OsNCl_4]^-$ is a d^2 complex the molecular orbitals are only filled to the $1b_2$ level. To understand why the $[OsNCl_4]^-$ molecule prefers θ to be 104.8° compared to 90.0° it is necessary to focus on how the energies of the occupied molecular orbitals change with θ.

The 4e and 1e orbitals correspond to π bonding between the nitride and osmium and are localized on the nitride ligand. The chloride ligands also contribute to these molecular orbitals. In 4e the chloride orbitals are out of phase with the d_{xz} and d_{yz} orbitals, and for the 1e orbitals the chloride orbitals are in phase with these d orbitals. The 3e and 4e orbitals are strongly localized on the chloride ligands. The 3e orbital has only a very small contribution from the metal and is out of phase with respect to metal–chloride bonding. The 2e orbital corresponds to in-phase overlap between the chlorides and the d_{xz} and d_{yz} orbitals of osmium.

The remaining two orbitals depicted in Fig. 2 are the $1a_1$ and $2a_1$. The latter corresponds to in-phase overlap between the osmium and the σ orbital of nitride. The $1a_1$ orbital is essentially a non-bonding orbital between the d_{z^2} orbital of osmium and the p_z orbitals of the chlorides.

The geometry of the $[OsNCl_4]^-$ molecule was allowed to relax from a 'flat' square pyramid (θ = 90.0°) to the optimized geometry in a stepwise fashion. The changes in the energies of the molecular orbitals are shown in a Walsh diagram (Fig. 3). The main energy changes occur for the $1a_1$ and occupied e orbitals of Fig. 2. The energy changes may be explained with regard to overlap changes between the constituent atomic orbitals of the molecular orbitals.

The 4e orbitals are antibonding with respect to the metals and the chlorides when θ = 90.0°. Increasing θ from 90.0° reduces the unfavourable overlap between the chloride π orbitals and the d_{xz} and d_{yz} orbitals, resulting in an overall stabilization of the 4e molecular orbitals. This is shown in **II**. The 3e orbitals increase in energy as the molecule relaxes to the optimized geometry. This is due to an increase in non-bonding repulsions as the equatorial chlorides bend away from nitrogen.[51] As θ increases the energy difference of the 4e and 3e orbitals becomes smaller and they eventually produce the 3e and 4e orbitals of the optimized structure shown in **III**. There is a net change in energy of the 3e and 4e orbitals of −1.0 eV as θ changes from 90.0 to 104.8°. The 2e and 1e orbitals decrease and increase in energy respectively as θ increases. Once again this may be accounted for by the change in overlaps within each molecular orbital **IV** and **V**. The resultant molecular orbitals in the optimized structure, 1e and 2e, are shown in **VI**. The variation of θ results in a net destabilization of the 1e and 2e orbitals of 0.46 eV.

Finally, the other major energy change occurs for the $1a_1$ orbital. At 90.0° this orbital is non-bonding between the metal and the chloride ligands (see Fig. 2). As θ is increased from 90.0° the chloride moves towards the nodal plane of the d_{z^2} orbital. This increases the π interaction between the chloride orbitals and the d_{z^2} orbital (see **VII**). This interaction stabilizes the energy of this molecular orbital by 0.38 eV.

In summary, the π interactions between the metal and the nitride are stabilized as θ increases from 90 to 104.8°. In addition, there is a decrease in out-of-phase π interactions between the metal and the basal chlorides.

Orbital and steric interaction energy analysis for $[OsNCl_4]^-$. In the previous section the electronic structure of $[OsNCl_4]^-$ was discussed. The way in which the energetics of the molecule varies as the structure of the molecule changes from the 'flat' square-pyramidal geometry (θ = 90.0°) to the optimized geometry is now considered. Using the transition-state method[30–33] the effects of orbital interactions and steric interactions on the geometry of $[OsNCl_4]^-$ may be quantitatively assessed. The total bonding energy of the molecule may be decomposed in equation (3). In general E_{steric} is destabilizing and E_{el} is stabilizing. In a previous section the change of θ from 90.0 to 104.8° was seen to result in a net stabilization of the molecular orbitals of $[OsNCl_4]^-$.

In Table 3 the values of the energy components of equation (3) are presented for $[OsNCl_4]^-$ with θ = 90.0 or 104.8°. It is found that E_{steric} is more destabilizing when the molecule has a 'flat' square-pyramidal geometry. Since the proximity of the nitride group to the other ligands is closer when θ = 90.0°, then

Table 3 Decomposition of the total bonding energy into steric interaction and orbital interaction components for $[OsNCl_4]^-$ with the angle of pyramidalization, θ (see **I** for definition)

	θ/°	
Energy/kJ mol^{-1}	90.0	104.8
ΔE_{steric}	3474.8	3357.0
ΔE_{el}	−6418.1	−6653.7
ΔE_b	−2943.3	−3296.7

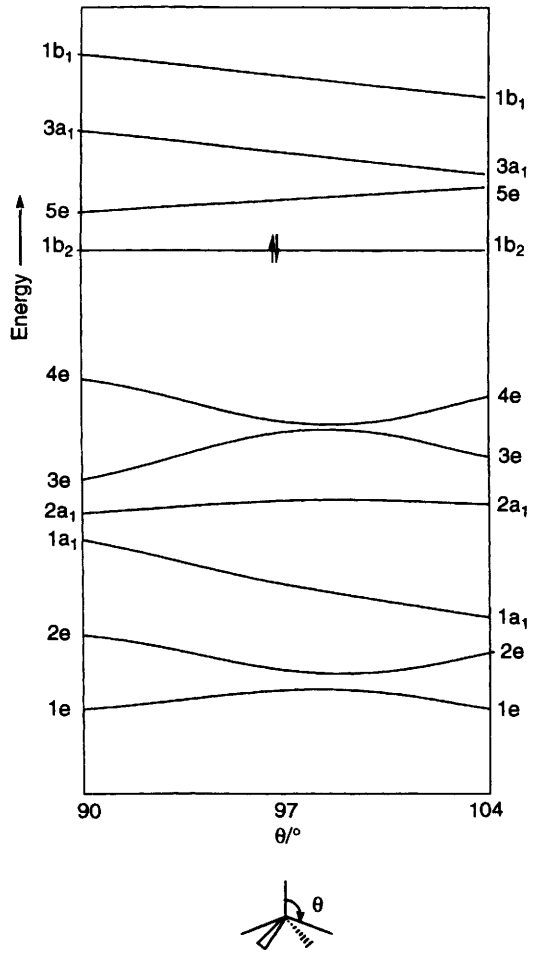

Fig. 3 Orbital energy changes of $[OsNCl_4]^-$ as θ is varied from 90 to 104°. The HOMO is indicated by an electron pair

the contribution to the total bonding energy from E_{steric} is expected to be larger. Opening θ to 104.8° reduces the destabilizing influence of steric interactions. This concurs with Bright and Ibers[10] assessment of the reduction of the steric energy of a molecule with an increase of the *trans* influence. However, it may also be seen from Table 3 that the orbital interaction energy, E_{el}, increases as θ is increased from 90.0 to 104.8°. The total change in E_{el} is -235.6 kJ mol^{-1}. Thus, both an increase in orbital interaction energy and a decrease in steric interaction energy occur when θ is increased from 90.0 to 104.8°. From Table 3 it may be seen that the stabilization conferred on the molecule by the increase in orbital interaction energy is much greater than the stabilization conferred by a decrease in steric interaction energy.

Different spectator ligands. The effect of altering the electronic nature of the spectator ligand was investigated. The chloride ligands of $[OsNCl_4]^-$ were substituted by strongly σ-donating alkyl groups and by thiolate groups. There have been X-ray characterizations of some $[MNX_4]^-$ complexes where X = alkyl or thiolate (see Table 1). The complexes $[OsNMe_4]^-$ and $[OsN(SMe)_4]^-$ were chosen as models for the alkyl and thiolate complexes. The optimized structures of the model complexes are given in Table 2. It may be seen that the angular distortion has not been diminished by substituting the chlorides by alkyl and thiolate groups. Indeed, it is larger than for $[OsNCl_4]^-$. In addition, the reactivities of $[OsNMe_4]^-$ and $[OsN(SMe)_4]^-$ are quite different. For the alkyl complex it has been found that phosphines react at the nitride group.[47] The thiolate complexes have been shown to react with electrophiles such as alkyl halides, with the sulfur atoms being the site of attack.[53]

The structural and reactivity differences of the alkyl and thiolate complexes compared to $[OsNCl_4]^-$ may be explained by comparing the nature of the molecular orbitals of these complexes. From the analysis of the geometric distortion of $[OsNCl_4]^-$ it was shown that osmium–nitride π-bonding orbitals were stabilized. Specifically, the 4e orbital of Fig. 2 decreases in energy as θ increases from 90.0°. This stabilization is counteracted by the destabilization of the 3e set of orbitals (see Fig. 3). In the alkyl complex there are no analogous orbitals retarding the stabilization of the metal–nitride bond since alkyl ligands have only one σ valence orbital. This allows θ to open out to a larger angle. In the thiolate complex the thiolate ligands have σ and π valence orbitals. However, the lower electronegativity of sulfur compared to chlorine means that there will be differences in orbital orderings compared to those of the $[OsNCl_4]^-$ complex. In $[OsNCl_4]^-$ the 4e orbital lies above the 3e (see Fig. 2). In $[OsN(SMe)_4]^-$ the ordering of these orbitals is reversed which may result in θ being able to open more in this complex.

The distinctive reactivities of $[OsNMe_4]^-$ and $[OsN(SMe)_4]^-$ may be explained by consideration of the frontier orbitals of these complexes. The lowest unoccupied molecular orbital (LUMO) of $[OsNMe_4]^-$ complex is shown in **VIII**. This orbital has been stabilized by opening θ from 90.0°. Since the alkyl group is a strong σ donor it makes an appreciable contribution to this orbital at the expense of the nitrido orbital. Moving the alkyl groups away from the nitride diminishes the overlap between the alkyl σ orbitals and the osmium d orbital. Since this orbital is unoccupied, and is located in the frontier region of the complex, then it is conceivable that Lewis bases could interact with this orbital at the nitrogen atom.

The opening of θ from 90.0 to 108.0° in $[OsN(SMe)_4]^-$ results in $1a_2$ (see **IX**) becoming the HOMO of the molecule. This orbital is a non-bonding orbital that is entirely localized on the sulfur atoms. The equivalent orbital of $[OsNCl_4]^-$ is much lower-lying due to the greater electronegativity of chlorine. Thus, the occupied $1a_2$ orbital of $[OsN(SMe)_4]^-$ means that electron density is high on the sulfur atoms in the frontier region and could easily provide a site for attack by an electrophile. While this analysis provides a rationalization for the sites of attack of electrophiles and nucleophiles on these molecules, further study is required to give an extensive analysis.

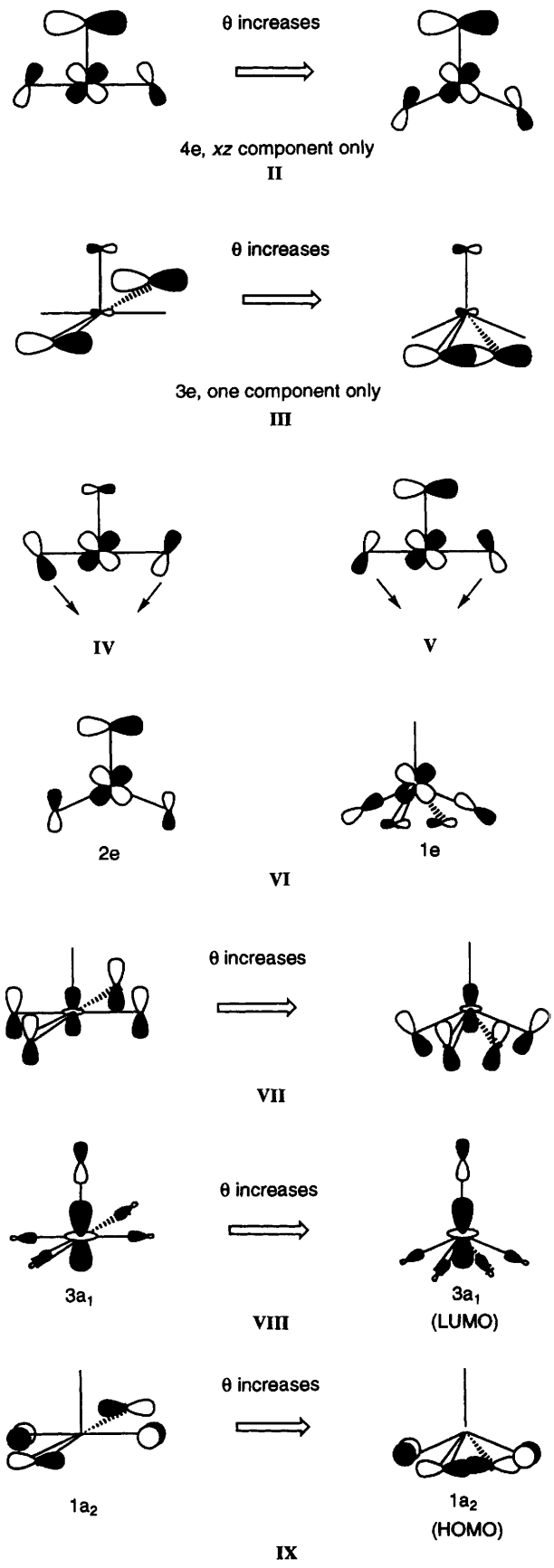

The Geometric and Electronic Structure of $[OsNCl_5]^{2-}$.—The optimized geometry for $[OsNCl_5]^{2-}$ is shown in Fig. 4.

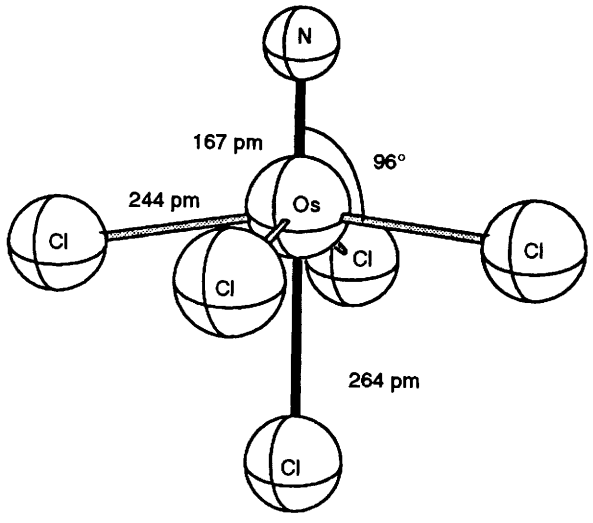

Fig. 4 Optimized geometry of $[OsNCl_5]^{2-}$

Again the calculation has satisfactorily reproduced the angular distortion observed in the experimental structure and the bond lengths are in good agreement with experiment,[10] although consistently slightly higher. The distortion of the basal angles away from the nitride ligand is not as pronounced as the distortion in $[OsNCl_4]^-$. The bond between the metal and the *trans* chloride is almost 20 pm longer than the bonds between the metal and the *cis* chlorides.

As for $[OsNCl_4]^-$ an analysis of the energy changes of the occupied molecular orbitals as a function of the angle θ may provide an explanation for the *trans* influence in $[OsNCl_5]^{2-}$. In particular, the smaller angular distortion in six- compared to five-co-ordinate systems, and the reason for the very long bond to the *trans* ligand. Once again θ is defined as the Cl–M–N angle in $[OsNCl_5]^{2-}$, as shown in **X**.

The main molecular orbitals of $[OsNCl_5]^{2-}$ with θ restricted to 90.0° are depicted in Fig. 5. There are many similarities between these and those of $[OsNCl_4]^-$ (θ = 90.0°, see Fig. 2), but there are also some important differences. The HOMO of $[OsNCl_5]^{2-}$ with a 'flat' square-pyramidal geometry is the $1b_2$ orbital corresponding to the out-of-phase interactions between the osmium d_{xy} orbital and the chloride p orbitals. Above this orbital is the 5e set which are the antibonding interactions between the osmium d_{xz} and d_{yz} orbitals and the nitrido π orbitals. The next highest orbital is the $1b_1$, corresponding to antibonding interactions between the $d_{x^2-y^2}$ osmium orbital and the chloride σ orbitals. The last four orbitals are virtually the same as the corresponding orbitals of $[OsNCl_4]^-$. However, the $3a_1$ orbital is different to the analogous orbital in the five-co-ordinate complex. Referral to Fig. 2 shows that in $[OsNCl_4]^-$ the $3a_1$ orbital is localized on an osmium hybrid orbital which is directed away from the nitride ligand. In $[OsNCl_5]^{2-}$ the σ orbital of the *trans* chloride overlaps with the $3a_1$ orbital of $[OsNCl_4]^-$. Thus the $3a_1$ orbital of $[OsNCl_5]^{2-}$ corresponds to the out-of-phase overlap of these two orbitals. The in-phase combination is low-lying and occupied. The 4e orbitals are seen to be very similar to those of $[OsNCl_4]^-$ (see Fig. 2). Recall that the 4e orbital played a key role as θ was increased from 90.0°. The $2a_1$ orbital is virtually non-bonding, and differs substantially from the analogous orbital of $[OsNCl_4]^-$.

Allowing θ to relax back to the optimized value results in energy changes to some molecular orbitals. In the case of $[OsNCl_4]^-$ the 4e orbitals were stabilized as θ increased, resulting in enhanced π overlap between the metal and the nitride ligand. Similarly, the 4e orbitals of $[OsNCl_5]^{2-}$ are stabilized as θ increases from 90.0°. In $[OsNCl_4]^-$ the stabilization of the 4e set was countered by a destabilization of

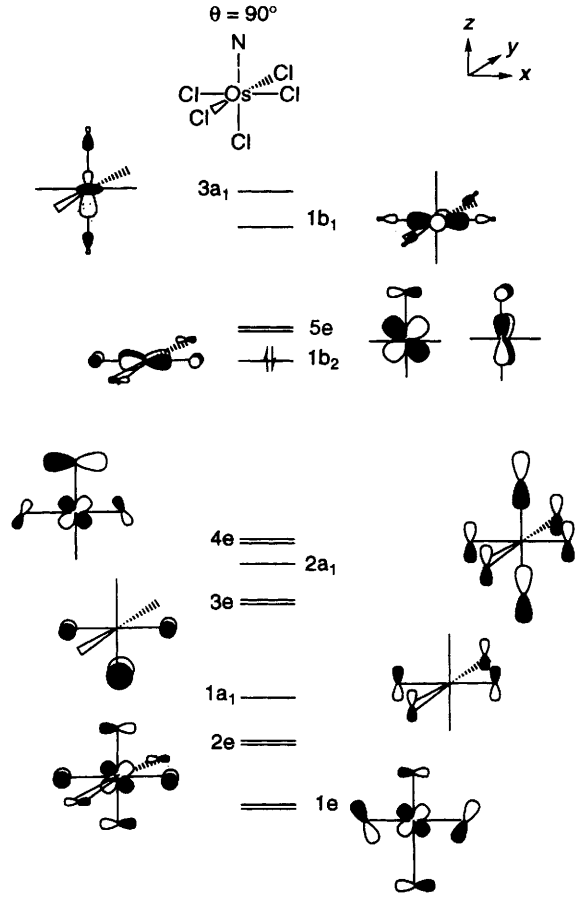

Fig. 5 Selected molecular orbitals of $[OsNCl_5]^{2-}$; details as in Fig 2

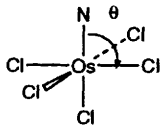

X

the 3e set. Once again, for $[OsNCl_5]^{2-}$ the 3e set is destabilized as θ relaxes to its optimized value. The extent of the destabilization of the 3e set with increasing θ is greater for $[OsNCl_5]^{2-}$ than for $[OsNCl_4]^-$. This is depicted in **XI**. The rate of increase in destabilization is greater in $[OsNCl_5]^{2-}$ due to stronger non-bonding repulsions.[51] This tempers the extent of the angular distortion in the six-co-ordinate complex. In addition the $2a_1$ orbital rapidly becomes destabilized as θ increases above 90.0°, as shown in **XII**. This orbital destabilization also controls the extent of the angular distortion in six-co-ordinate nitrido complexes. In addition, from **XII** it is apparent that it should also result in a lengthening of the bond from the metal to the *trans* chloride, in order to minimize the non-bonded repulsions between *cis* and *trans* chlorides.

Orbital and Steric Interaction Energy Analysis for $[OsNCl_5]^{2-}$.—The previous section indicated that the angular distortion in six-co-ordinate complexes is less than for five-co-ordinate nitrido complexes. In this section a decomposition of the energy of $[OsNCl_5]^{2-}$ is presented. The values of the steric and orbital interaction energies [see equation (3)] for $[OsNCl_5]^{2-}$ with θ = 90.0 and 95.0° are presented in Table 4.

The results are similar to those found for $[OsNCl_4]^-$. Both the changes in orbital and steric interaction energies stabilize the total bonding energy of the complex as θ increases from 90.0 to 95°. However, the relative magnitudes of the contributions

has changed in comparison to $[OsNCl_4]^-$. The orbital interaction energy is still the major contributor. Thus this analysis suggests that steric interaction energies have a secondary role to play in stabilizing the $[OsNCl_5]^{2-}$ molecule, as suggested by Bright and Ibers.[10] It increases as the ligands become bulkier as found for the rhenium complexes studied by those workers.

The Absence of a trans *Influence in Related Complexes.*— Apart from the complexes studied in the previous sections, many others, exhibit *trans* influences.[3] In these molecules the basal angles vary from 96 to 110°.[3] Nonetheless there are some examples of related complexes which do not show a *trans* influence. While the nitrogen based ligands, nitride, imide and hydrazide exert *trans* influences,[3] the linear nitrosyl complexes are not noted for geometric distortions as a consequence of a *trans* influence.[54] Consider $[Ru(NO)Cl_5]^{2-}$, the nitrosyl analogue of $[OsNCl_5]^{2-}$. This complex has octahedral coordination and has neither an unusually long *trans* Ru–Cl bond nor angular distortion away from the nitrosyl group.[55] In the previous sections we have established that the distortions in $[OsNCl_5]^{2-}$ and $[OsNCl_4]^-$ are governed primarily by stabilizing orbitals involved in metal–nitrogen π bonding. Therefore, the question of the absence of a *trans* influence in $[Ru(NO)Cl_5]^{2-}$ may be related to the extent of bonding between the metal and nitrosyl (a π acceptor) valence orbitals.

In Fig. 6 the calculated optimized structure for $[Ru(NO)Cl_5]^{2-}$ is illustrated. The agreement with experiment[55] is very good. The bond distances compare well with the experimental values. The nitrosyl to ruthenium bond length is typical of transition metal–nitrosyl complexes.[54] The *cis* Ru–Cl bonds are calculated to be 2 pm shorter than the bond to the *trans* chloride. A slight distortion of the angles from ideal octahedral geometry is calculated with the N–Ru–Cl_{cis} angle calculated to be 91.2°. This is only a very slight distortion and should not be considered the result of a strong *trans* influence.

There have been many theoretical studies of nitrosyl complexes[50] and the valence orbitals of a linear nitrosyl ligand are well defined as a lone-pair σ-donor orbital and a higher-lying pair of π*-acceptor orbitals. There is nothing remarkable about the electronic structure of $[Ru(NO)Cl_5]^{2-}$, however, selected frontier orbitals of this complex are shown in Fig. 7 in order to aid the following discussion. Both the d_{z^2} and $d_{x^2-y^2}$ orbitals enter into strong σ interactions with the ligands resulting in the $2a_1$ and $1b_1$ orbitals shown in Fig. 7. The t_{2g} type orbitals on ruthenium are separated in energy by the interactions of the d_{xz} and d_{yz} orbitals with the π* orbitals on the nitrosyl ligand. The bonding and antibonding interactions of the d_{xz} and d_{yz} orbitals of ruthenium with the π* orbitals of

Table 4 Decomposition of the total bonding energy for $[OsNCl_5]^{2-}$ with θ (see **II** for definition)

	θ/°	
Energy/kJ mol^{-1}	90.0	96.0
ΔE_{steric}	3655.2	3626.1
ΔE_{el}	−6872.0	−6923.4
ΔE_b	−3216.8	−3297.3

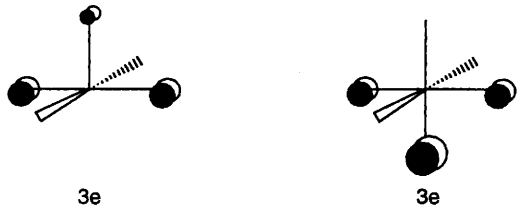

XI

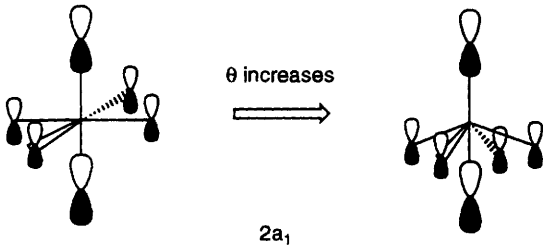

XII

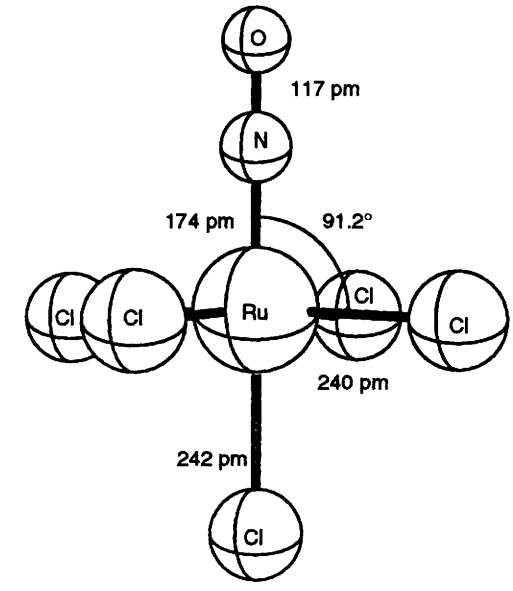

Fig. 6 Optimized geometry of $[Ru(NO)Cl_5]^{2-}$

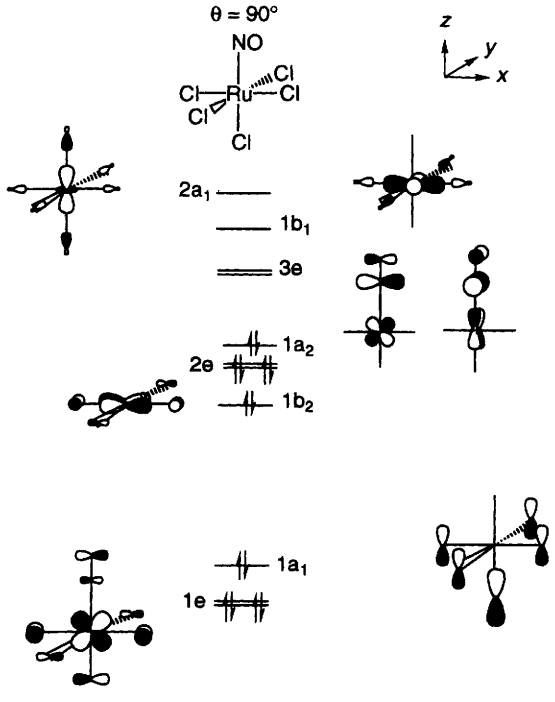

Fig. 7 Frontier interactions of $[Ru(NO)Cl_5]^{2-}$

the nitrosyl result in the 1e and 3e orbitals. The d_{xy} orbital interacts with the chlorides to form the $1b_2$ orbital. The HOMO of the complex is a non-bonding $1a_2$ orbital localized entirely on the equatorial chloride ligands. Finally, below the HOMO lie the 2e orbitals, which are predominantly localized on the chloride ligands.

If the structure of $[Ru(NO)Cl_5]^{2-}$ was distorted in a similar manner to $[OsNCl_5]^{2-}$ it is expected that hybridization would take place to orientate the d_{xz}/d_{yz} pair toward the nitrosyl ligand. Hybridizing these orbitals to the nitrogen should increase this overlap with the nitrosyl π^* orbital. The difference now is that this interaction weakens an existing bond on the nitrogen ligand (the N–O π bond) which did not happen in the case of the nitride ligand.

To confirm these predictions we decided to perform a partial optimization of the $[Ru(NO)Cl_5]^{2-}$ complex, fixing the N–Ru–Cl_{cis} angles at 95°. The partially optimized geometry of the distorted $[Ru(NO)Cl_5]^{2-}$ complex is shown in Fig. 8. There are several features to note. First, the bond between the *trans* chloride and ruthenium has been weakened, increasing in length by 30 pm. Secondly, the bonds to the *cis* chlorines have also been weakened due to diminished overlap of these ligands with the $d_{x^2-y^2}$ orbital. Thirdly, the ruthenium to nitrogen bond has shortened slightly which is consistent with an increased overlap between the nitrosyl and ruthenium orbitals. Finally, a corollary of the increased overlap between the metal and nitrosyl ligands is the very long N–O bond of the nitrosyl. A Mulliken population analysis of the complex in both geometries shows that there is an increase in the population of the nitrosyl π^* orbitals as the basal chlorides bend away from the nitride ligand, from 0.59 in the optimized structure to 0.93 in the distorted complex. All of these features confirm the trends predicted for this distortion.

In addition, the energies of the molecular orbitals depicted in Fig. 7 have changed. The 1a occupied orbital has been destabilized (see **XIII**). The 3e orbital has also increased in energy indicating an increased overlap between the metal orbitals and the π^* orbitals of the nitrosyl group.

The orbital interaction and steric energies for $[Ru(NO)Cl_5]^{2-}$ with the experimental and distorted geometries are given in Table 5. These results show that the orbital interaction energy decreases as the $[Ru(NO)Cl_5]^{2-}$ molecule is distorted from its ground-state structure to the partially optimized geometry with $\theta = 95.0°$. This confirms the molecular orbital analysis given above. The steric interaction is seen to decrease as θ bends, but does not compensate for the loss in orbital interaction energy. Overall, the distortion is destabilizing for the molecule.

Hence, there are several factors inhibiting the *trans* influence in $[Ru(NO)Cl_5]^{2-}$. First increasing the π overlap between the nitrosyl and the metal orbitals increases the population of the nitrosyl π^* orbital. In the nitrido complexes the M≡N bond strengthened as θ increased from 90.0°. In the nitrosyl complex the M–N bond also strengthens as θ increases, but now the N–O bond weakens. Secondly, increasing θ from the optimized value to 95.0° in the nitrosyl complex results in a destabilization of chloride-based molecular orbitals. Thus, taken together, the destabilizing factors outweigh the stabilizing factors which results in an absence of a *trans* influence in $[Ru(NO)Cl_5]^{2-}$.

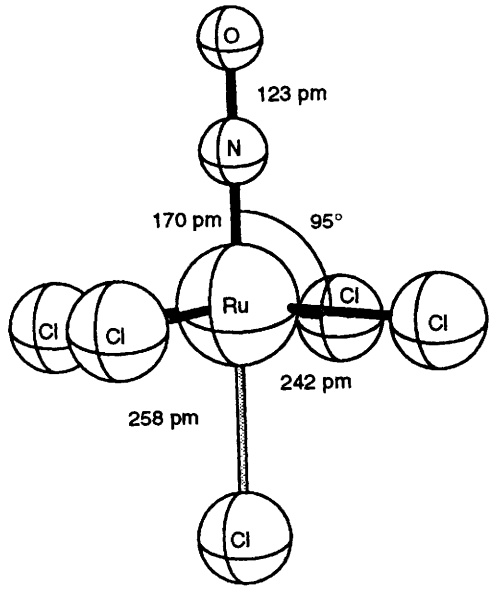

Fig. 8 Partially optimized geometry of $[Ru(NO)Cl_5]^{2-}$ with the N–Ru–Cl angle kept at 95°

Conclusion

The theoretical geometries of $[OsNX_4]^-$ (X = Cl, Me or SMe) and $[OsNCl_5]^{2-}$ have been determined and there is good agreement between the calculated and experimental structures. This study has quantitatively established the relative importance of the roles played in the *trans* influence of these complexes by steric and electronic factors. The decrease in steric interaction energy and the increase in orbital interaction energy both contribute to the presence of a *trans* influence in five- and six-co-ordinate nitrido complexes. In five-co-ordinate complexes the contribution from the change in orbital interaction energy is much greater than that from the change in steric interaction energy. In six-co-ordinate complexes the relative contributions of orbital and steric interactions are the same, but the differences in their magnitudes are smaller.

In six-co-ordinate complexes switching the *trans* influencing ligand from a strong π donor to a π acceptor results in an absence of a *trans* influence. This may be rationalized from an orbital viewpoint by an increase in destabilizing interactions as θ increases from 90.0°.

Substituting the spectator ligand X in $[OsNX_4]^-$ from chloride to an alkyl and a thiolate group was found not to affect the extent of the *trans* influence in these complexes. A brief consideration of the frontier regions indicates that the alkyl complex is predicted to be amenable to reactions with Lewis bases at the nitrogen atom, and the thiolate complex is predicted to be susceptible to electrophilic attack at the sulfur atoms. These findings are in concordance with experimental results.[47,54]

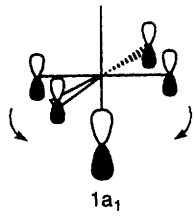

XIII

Table 5 Decomposition of the total bonding energy for $[Ru(NO)Cl_5]^{2-}$ with $\theta = 91.2$ (optimized geometry) and 95.0° (partially optimized structure); see **II** or **X** for definition of θ

	θ/°	
Energy/kJ mol^{-1}	91.2	95.0
ΔE_{steric}	6179.7	5798.7
ΔE_{el}	−9791.4	−9390.3
ΔE_b	−3611.7	−3591.5

Acknowledgements

We thank Professor Tom Ziegler for the use of his computing facilities at the University of Calgary and both him and Heiko Jacobsen for many helpful discussions. The British Council is thanked for a studentship (to P. D. L.).

References

1 A. Pidcock, R. E. Richards and L. M. Venanzi, *J. Chem. Soc. A*, 1966, 1707.
2 T. G. Appleton, H. C. Park and L. E. Manzer, *Coord. Chem. Rev.*, 1973, **10**, 335.
3 W. A. Nugent and J. M. Mayer, *Metal Ligand Multiple Bonds*, Wiley, New York, 1988.
4 A. A. Grinberg, *Acta Physicochim. URSS*, 1935, **3**, 573.
5 Y. K. Syrkin, *Izv. Akad. Nauk SSSR, Otd. Khim. Nauk*, 1948, 69.
6 J. Chatt, L. A. Düncouson and L. M. Venanzi, *J. Chem. Soc.*, 1955, 4456.
7 L. F. Orgel, *J. Inorg. Nucl. Chem.*, 1956, **2**, 137.
8 E. M. Shustorovich, M. A. Porai-Koshits and Yu. A. Buslaev, *Coord. Chem. Rev.*, 1975, **17**, 1.
9 J. K. Burdett and T. A. Albright, *Inorg. Chem.*, 1979, **18**, 2112.
10 D. Bright and J. A. Ibers, *Inorg. Chem.*, 1969, **8**, 709.
11 P. W. R. Corfield, R. J. Doedens and J. A. Ibers, *Inorg. Chem.*, 1967, **6**, 197.
12 R. J. Doedens and J. A. Ibers, *Inorg. Chem.*, 1967, **6**, 204.
13 R. G. Parr and W. Yang, *Density Functional Theory of Atoms and Molecules*, Oxford University Press, New York, 1989.
14 T. Ziegler, *Chem. Rev.*, 1991, **91**, 651.
15 O. Gunnarsson and I. Lundquist, *Phys. Rev. B*, 1974, **10**, 1319.
16 O. Gunnarsson and I. Lundquist, *Phys. Rev. B*, 1976, **13**, 4274.
17 O. Gunnarsson, M. Johnson and I. Lundquist, *Phys. Rev. B*, 1979, **20**, 3136.
18 H. Stoll, C. M. E. Pavlidou and H. Preuss, *Theor. Chim. Acta*, 1978, **49**, 143.
19 H. Stoll, E. Golka and H. Preuss, *Theor. Chim. Acta*, 1980, **55**, 29.
20 S. J. Vosko, M. Wilk and M. Nusair, *Can. J. Phys.*, 1980, **58**, 1200.
21 E. J. Baerends, D. E. Ellis and P. Ros, *Chem. Phys.*, 1973, **2**, 41.
22 E. J. Baerends, Ph. D. Thesis, Vrije Universitet, Amsterdam, 1975.
23 W. Ravenek, *Algorithms and Applications on Vector and Parallel Computers*, eds. H. J. J. Riele, Th. J. Dekker and H. A. van de Vorst, Elsevier, Amsterdam, 1987.
24 P. M. Boerrigter, G. te Velde and E. J. Baerends, *Int. J. Quantum Chem.*, 1988, **33**, 87.
25 G. J. Snijders, E. J. Baerends and P. Vernooijs, *At. Data Nucl. Data Tables*, 1982, **26**, 483.
26 P. Vernooijs, G. J. Snijders and E. J. Baerends, *Slater Type Basis Functions for the whole Periodic System*, Internal report, Free University of Amsterdam, 1981.
27 J. Krijn and E. J. Baerends, *Fit functions in the HFS-method*, Internal report, Free University of Amsterdam, 1984.
28 A. D. Becke, *J. Chem. Phys.*, 1986, **84**, 4524.
29 J. P. Perdew, *Phys. Rev. B*, 1986, **33**, 8822.
30 T. Ziegler and A. Rauk, *Theor. Chim. Acta*, 1977, **46**, 1.
31 E. J. Baerends and A. Rozendaal, *NATO ASI, Ser. C*, 1986, **176**, 159.
32 T. Ziegler and A. Rauk, *Inorg. Chem.*, 1979, **18**, 1558.
33 T. Ziegler, *NATO ASI, Ser. C.* 1992, **378**, 367.
34 T. Ziegler, V. Tschinke and C. Ursenbach, *J. Am. Chem. Soc.*, 1987, **109**, 4825.
35 H. Jacobsen, H.-B. Kraatz, T. Ziegler and P. M. Boorman, *J. Am. Chem. Soc.*, 1992, **114**, 7851.
36 J. Li, G. Schrechenbach and T. Ziegler, *J. Phys. Chem.*, 1994, **98**, 4838.
37 T. Ziegler and J. Li, *Can. J. Chem.*, 1994, **72**, 783.
38 H. Jacobsen and T. Ziegler, *J. Am. Chem. Soc.*, 1994, **116**, 3667.
39 L. Versluis and T. Ziegler, *J. Chem. Phys.*, 1988, **88**, 322.
40 C.-M. Che and V. W.-W. Yam, *Adv. Inorg. Chem.*, 1992, **39**, 233.
41 U. Müller, E. Schweda and J. Strähle, *Z. Naturforsch., TeilB*, 1983, **38**, 1299.
42 J. Baldas, J. F. Boas, J. Bonnyman and G. A. Williams, *J. Chem. Soc., Dalton Trans.*, 1984, 2395.
43 W. Kafitz, F. Weller and K. Dehnicke *Z. Anorg. Allg. Chem.*, 1982, **490**, 175.
44 F. L. Phillips and A. C. Skapski, *Acta Crystallogr., Sect. B*, 1975, **31**, 2667.
45 F. L. Phillips and A. C. Skapski, *J. Cryst. Mol. Struct.*, 1975, **5**, 83.
46 J. Baldas, J. Bonnyman, P. M. Pojer, G. A. Williams and M. F. MacKay, *J. Chem. Soc., Dalton Trans.*, 1981, 1798.
47 P. A. Shapley and Z. -Y. Own, *Organometallics*, 1986, **5**, 1269.
48 P. A. Shapley, H. sik Kim and S. R. Wilson, *Organometallics* 1988, **7**, 928.
49 K. Dehnicke, J. Schmitte and D. Fenske, *Z. Naturforsch., Teil B*, 1980, **35**, 1070.
50 A. R. Rossi and R. Hoffmann, *Inorg. Chem.*, 1975, **14**, 365.
51 J. T. Veal and D. J. Hodgson, *Inorg. Chem.*, 1972, **11**, 1420.
52 D. L. Dubois and R. Hoffmann, *New J. Chem.*, 1977, **1**, 425.
53 C. J. Balhausen and H. B. Gray, *Inorg. Chem.*, 1962, **1**, 111.
54 N. Zhang, S. R. Wilson and P. A. Shapley, *Organometallics*, 1988, **7**, 1126.
55 D. M. P. Mingos and D. J. Sherman, *Adv. Inorg. Chem.*, 1989, **34**, 293.

Received 27th September 1994; *Paper* 4/05903D